RSC Advances

PAPER

View Article Online
View Journal | View Issue

Cite this: *RSC Adv.*, 2023, **13**, 35359

Study on the effect of an ultrasound assisted reaction on the crystallization properties of recovered cryolite

Chenchen Wang [abc] and Song Mao*[abc]

During the treatment of spent cathode carbon from electrolytic aluminum, a large amount of fluoride containing wastewater is generated. By adding different sodium source and aluminum source reagents, under the conditions of different addition order, pH, temperature and time, the effects of conventional static reaction, stirring reaction and ultrasonic assisted reaction on the crystallization properties of recovered cryolite were investigated. The results showed that under the optimum reaction conditions (sodium source: NaCl, aluminum source: $AlCl_3$, the molar ratio of $AlCl_3$ to NaCl is 1 : 3, addition order: first addition of $AlCl_3$ and then NaCl, pH is 8.57, time is 40 min, temperature at room temperature), the removal efficiency of fluoride ions was the highest when ultrasound assisted treatment was used. The cryolite products with ultrasound assisted crystallization and without ultrasound assisted crystallization were characterized using SEM and TEM. The results showed that the crystal particles obtained by ultrasound assisted crystallization were relatively concentrated, and the morphology was regular and the surface was smooth. Design Expert orthogonal software was used to design the response surface test, it was found that ultrasound time has the most significant impact on the content of recovered cryolite among single factors, and the interaction between ultrasound frequency and ultrasound power, ultrasound power and ultrasound time was highly significant among multiple factors.

Received 30th September 2023
Accepted 29th November 2023

DOI: 10.1039/d3ra06661d

rsc.li/rsc-advances

1. Introduction

In recent years, the electrolytic aluminum industry has developed rapidly, and at the same time, the production of dangerous by-product spent cathode carbon (SCC) is also increasing.[1,2] Due to the continuous erosion of cathode carbon by high-temperature electrolytes, molten aluminum, sodium salts and other substances during the production process, its service life is shortened to 5–8 years.[3,4] SCC contains many valuable inorganic compounds, such as alumina, cryolite, fluoride, and aluminum silicate, and some carbon blocks also contain small amounts of cyanide.[5,6] According to statistics, 30–50 kg of spent cathode carbon will be produced for every 1 t of aluminum production.[7] In the past, SCC was usually directly landfill treated.[8] However, since the fluoride in SCC can penetrate the soil and pollute groundwater, which has a great impact on the health and ecological balance of animals and plants,[9,10] many countries have listed SCC as a hazardous solid waste.[11] Therefore, achieving harmless treatment and resource utilization of SCC is an urgent problem to be solved in the electrolytic aluminum industry.

The commonly used methods for the treatment of spent cathode carbon include flotation method,[12] soluble aluminum salt solution leaching method,[13] acid leaching method[14,15] and alkali leaching method.[16] However, these methods generate a large amount of high concentration fluoride wastewater during the treatment process, which has become a thorny problem.[17,18] The common treatment methods for fluoride containing wastewater include chemical precipitation method,[19] coagulation precipitation method,[20] crystallization precipitation method,[21] adsorption method,[22] ion exchange method,[23] *etc.* Some methods have problems such as complex equipment, large operating capacity, high energy consumption, and high treatment cost in the treatment process, making it difficult to be widely applied.[24,25] The chemical precipitation method is widely used in industry due to its low treatment cost, good effect, and simple operation.[26] The most common method is to treat industrial fluoride containing wastewater by adding bleaching powder, ultimately generate calcium fluoride precipitation to remove fluoride ions.[27] However, the chemical treatment process produces a large amount of waste residue, which is difficult to precipitate, and the value of the recovered products is low.

In response to these shortcomings, this experiment uses the crystallization method to treat high concentration fluoride

[a]*Mining College, Guizhou University, Guiyang 550025, China*
[b]*National & Local Joint Laboratory of Engineering for Effective Utilization of Regional Mineral Resources from Karst Areas, Guiyang 550025, China*
[c]*Guizhou Key Laboratory of Comprehensive Utilization of Nonmetallic Mineral Resources, Guiyang 550025, China. E-mail: gzsongm@126.com*

containing wastewater generated during the treatment of spent cathode carbon. Single factor experiments are conducted to investigate the effects of reagent type, reagent addition order, solution pH, temperature, and time on the removal efficiency of fluoride ions. Characterization tests are also conducted to investigate the crystallization performance of recovered cryolite under static treatment, stirring treatment, and ultrasonic treatment conditions, in order to provide an efficient and valuable treatment method for fluoride containing wastewater.

2. Experiment

2.1 Experimental materials

The wastewater sample used in the experiment comes from high concentration fluoride containing wastewater after the treatment of electrolytic aluminum spent cathode carbon, with a fluoride ion content of approximately 2000 mg L^{-1}. All reagents use analytical pure reagents that meet national standards. Sodium hydroxide and sodium chloride were obtained from Chengdu Jinshan Chemical Reagent Co., Ltd. Sodium carbonate and aluminum chloride were obtained from Tianjin Yongda Chemical Reagent Co., Ltd. Sodium metaaluminate was obtained from Tianjin Damao Chemical Reagent Factory. Aluminum oxide was obtained from Shanghai McLean Biochemical Technology Co., Ltd. Hydrochloric acid was obtained from Chongqing Chuandong Chemical Co., Ltd. The experimental water was deionized water.

2.2 Experimental methods and procedures

100 mL of fluoride containing wastewater is taken in a polytetrafluoroethylene beaker. Under three reaction states of static conditions, stirring conditions and ultrasonic conditions, conduct a single factor experiment to investigate the effects of different sodium source reagents and aluminum source reagents, reagent addition order, solution pH, temperature, and time on the removal efficiency of fluoride ions. The experimental design is shown in Table 1. The experimental principle is shown in formula (1):

$$Al(OH)_4^- + 4H^+ + 3Na^+ + 6F^- \rightarrow Na_3AlF_6\downarrow + 4H_2O \quad (1)$$

The solution after the reaction was filtered. The filtrate was cooled and the residual fluoride ion in the filtrate was determined by the National Environmental Protection Standard HJ 488-2009 "Water quality – Determination of fluoride – Fluorine reagent spectrophotometric method". The detection principle is that fluoride ions react with fluoride reagent and lanthanum nitrate in an acetate buffer medium with a pH value of 4.1 to form a blue ternary complex. The absorbance of the complex at a wavelength of 620 nm is directly proportional to the concentration of fluoride ions, and fluoride is quantitatively measured (calculated as F^-). The solid obtained by filtration under the optimum conditions was dried and characterized by XRD, SEM and TEM.

The experiment was repeated three times under each experimental condition, and the removal efficiency of fluoride ion was calculated by the following formula (2):

$$\theta = \frac{2000 - \gamma}{2000} \quad (2)$$

In the formula, θ is the removal efficiency of fluorine ion (%), γ is the fluoride ion content of fluoride containing wastewater after treatment, and 2000 is the fluorine ion content (mg L^{-1}) in the raw material of fluoride containing wastewater.

2.3 Equipment and characterization

This section lists the equipment and characterization methods required for the experiments.

The pH of the solution was adjusted by pH meter (PHS-25, Shanghai Yidian Scientific Instrument, China). The solution was filtered in suction filter (SHB-111, Baoling Equipment, China). The fluoride containing wastewater was treated by ultrasonic equipment (KQ-600KDE, Kunshan Ultrasonic Instrument, China). The fluoride containing wastewater was heated and stirred by digital constant temperature stirring water bath (HH-6, Shanghai Shangpu Instrument & Equipment,

Table 1 Single factor test

Single factor experiment	Sodium source and aluminum source	Reagent addition order	pH	Temperature/°C	Time/min	Others
Group 1	**NaCl + $AlCl_3$, NaCl + Al_2O_3, NaCl + $NaAlO_2$, Na_2CO_3 + $AlCl_3$, Na_2CO_3 + $NaAlO_2$, NaOH + $AlCl_3$, NaOH + Al_2O_3, NaOH + $NaAlO_2$**	Adding together	8.57	Room temperature	30	Ultrasonic power 420 W, ultrasonic frequency 40 kHz, water bath stirring speed 480 rpm
Group 2	Optimal reagent combination	**$AlCl_3$ first then NaCl, NaCl first then $AlCl_3$, $AlCl_3$ and NaCl together**	8.57	Room temperature	30	
Group 3	Optimal reagent combination	Optimal order of addition	**0.75, 2.64, 5.34, 8.57, 11.66**	Room temperature	30	
Group 4	Optimal reagent combination	Optimal order of addition	Optimal pH	**25, 40, 55, 70, 85**	30	
Group 5	Optimal reagent combination	Optimal order of addition	Optimal pH	Optimal reaction temperature	**20, 40, 60, 80, 100**	

China). The deionized water used in the experiment was prepared by a distilled water generator (RO-DI-20L, Jin Feilan Water Treatment Equipment, China). The fluoride containing wastewater was tested by ultraviolet spectrophotometer (TU-1901, Beijing Persee General Instrument, China). The particle size distribution of synthetic cryolite was analyzed by particle size analyzer (LS13320, Beckman, USA). The composition of synthetic cryolite was analyzed by X-ray diffractometer (XRD) (D8 Advance, Bruker, Germany). The surface morphology of synthetic cryolite was observed by scanning electron microscopy (SEM) (Sigma 300, Zeiss, Germany). The internal structural distribution of synthetic cryolite was observed by transmission electron microscopy (TEM) (JEM-2100Plus, JEOL, Japan).

3. Results and discussion

3.1 Treatment experiment of fluoride containing wastewater

The addition of different sodium and aluminum sources will have different effects on the removal efficiency of fluoride ions, reaction time, and crystallization rate of cryolite in the solution. Therefore, it is crucial to find the optimal sodium and aluminum sources. The reagents were added according to the molar ratio of each element in the cryolite molecule. The molar ratio of aluminum sources to sodium sources is 1 : 3, so the addition amount of each reagent combination are as follows: NaCl 0.461 g + $AlCl_3$ 0.351 g, NaCl 0.461 g + Al_2O_3 0.134 g, NaCl 0.307 g + $NaAlO_2$ 0.216 g, Na_2CO_3 0.418 g + $AlCl_3$ 0.351 g, Na_2CO_3 0.279 g + $NaAlO_2$ 0.216 g, NaOH 0.316 g + $AlCl_3$ 0.351 g, NaOH 0.316 g + Al_2O_3 0.134 g, NaOH 0.211 g + $NaAlO_2$ 0.216 g.

As shown in Fig. 1, there is a significant difference in the removal efficiency of fluoride ions under different reagent combinations. When using NaCl + $NaAlO_2$ combination, the removal efficiency of fluoride ions in the three reaction states are the lowest, with 77.6%, 79.5%, and 80.9%, respectively; on the contrary, when NaCl + $AlCl_3$ combination is used, the removal efficiency of fluoride ions in all three reaction states are the highest, with 91.5%, 92.3%, and 94.7%, respectively. The removal efficiency of other reagent combinations is not high, the main reasons are as follows: (1) under neutral conditions, Al_2O_3 is difficult to dissociate aluminum ions, making it difficult to generate cryolite; (2) the addition of Na_2CO_3 and NaOH changes the pH of the solution, which is not conducive to the optimal environment for the formation of cryolite and affects the removal efficiency of fluoride ions; (3) $NaAlO_2$ only produces aluminum ions in strong acid solutions and does not react in weakly alkaline environments. Therefore, the best sodium source reagents and aluminum source reagents are NaCl and $AlCl_3$, respectively, and under this combination of reagents, the removal efficiency of fluoride ions with ultrasonic assistance is the highest, reaching 94.7%.

The type and dosage of reagents have been determined. The effect of the reagent addition order on the removal efficiency of fluoride ions was investigated under different reaction conditions. As shown in Fig. 2, when $AlCl_3$ is added first and then NaCl, the removal efficiency of fluoride ions in all three reaction states are the highest, with 92.7%, 94.7%, and 95%, respectively. On the contrary, when $AlCl_3$ and NaCl are added simultaneously, the removal efficiency of fluoride ions in all three reaction states are the lowest, at 90.4%, 93.7%, and 93.9%, respectively.

The reason is that adding $AlCl_3$ first can promote its hydrolysis in solution to generate $Al(OH)_4^-$. After its sufficient hydrolysis, adding sodium chloride can quickly form cryolite crystals. From this, it can be seen that adding $AlCl_3$ first and then NaCl can improve the crystallization rate of cryolite, and under ultrasonic assistance, the removal efficiency of fluoride ions is the highest, reaching 95%.

The effects of pH on the removal efficiency of fluoride ions in three reaction states were investigated by adjusting the pH of the solution to 0.75, 2.64, 5.34, 8.57, 11.66, respectively. From Fig. 3, it can be seen that under the five pH conditions, when the pH is 8.57, the removal efficiency of fluoride ions in all three reaction states are the highest, with 93.9%, 94.9%, and 95.5%, respectively. At pH of 0.75, the removal efficiency of fluoride

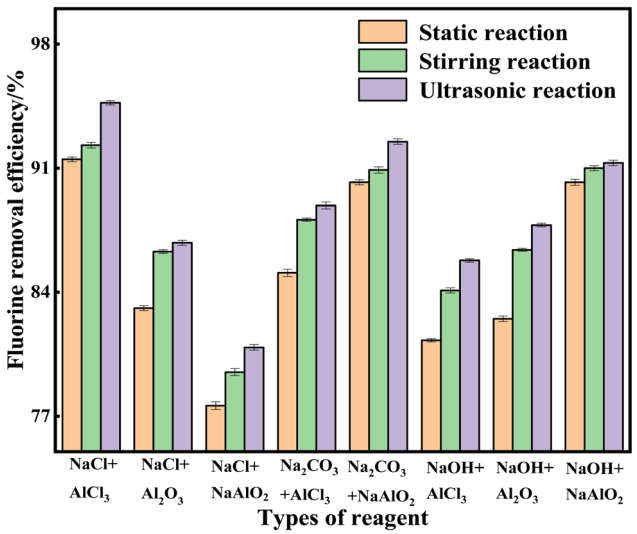

Fig. 1 Combination of different reagents.

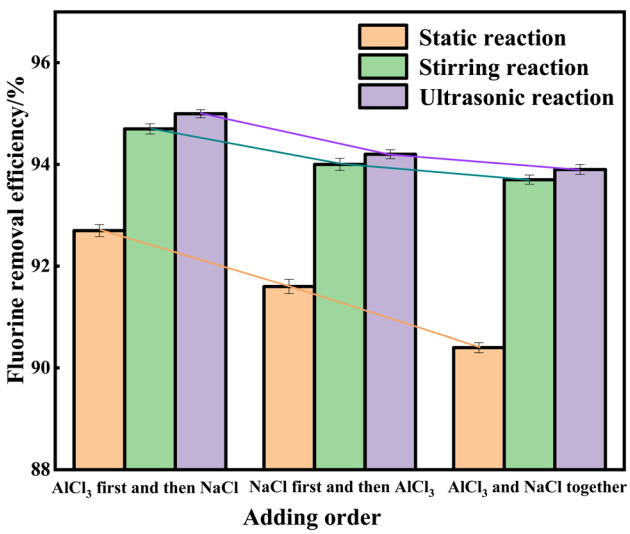

Fig. 2 The order of adding reagents.

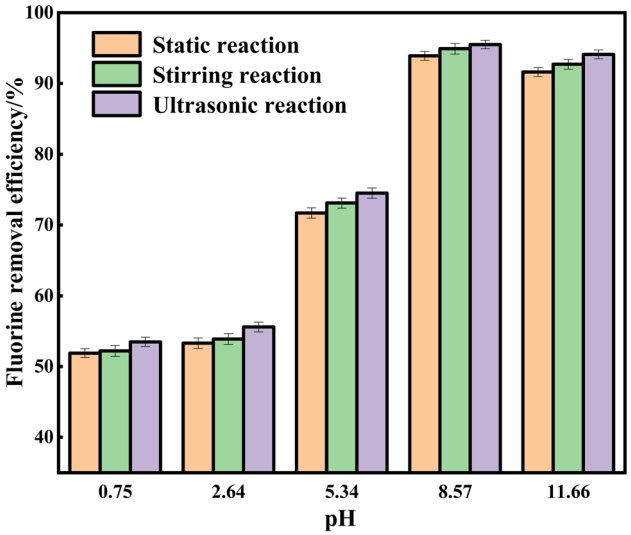

Fig. 3 The results under different pH conditions.

ions in all three reaction states are the lowest, with 51.9%, 52.2%, and 53.5%, respectively.

Due to cryolite will form different forms of aluminate solution under higher or lower pH conditions. In acidic environments, the main precipitate generated is $Al(OH)_3$; in a strongly alkaline environment, the formation of cryolite is accompanied by the formation of $AlF_3 \cdot 3H_2O$ precipitation. This conclusion has been previously studied by the team.[17]

Therefore, strong acid and alkali environments are not conducive to the formation of cryolite. The removal effect of fluoride ions is best in pH 8.7, and the highest fluoride ion removal efficiency is 95.5% when ultrasonic assisted.

The effects of different temperatures on the removal efficiency of fluoride ions under three different reaction states were investigated. From Fig. 4, it can be seen that under the static reaction state, the removal efficiency of fluoride ions is the highest at a temperature of 40 °C, which is 94.1%; under the stirring reaction state, the highest removal efficiency of fluoride ions is 94.9% at a temperature of 25 °C; in the ultrasonic reaction state, at temperatures of 25 °C and 40 °C, the removal efficiency of fluorine is consistently the highest, at 95.5%. From the figure, it can be seen that the removal efficiency at different temperatures do not differ significantly, and the synthesized cryolite is

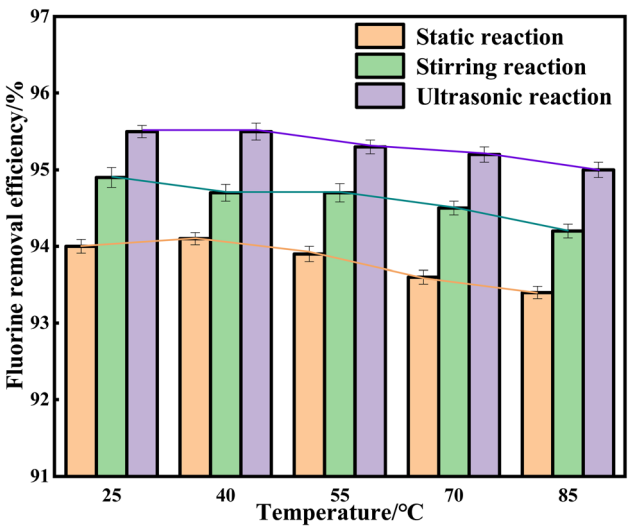

Fig. 4 The results under different temperature conditions.

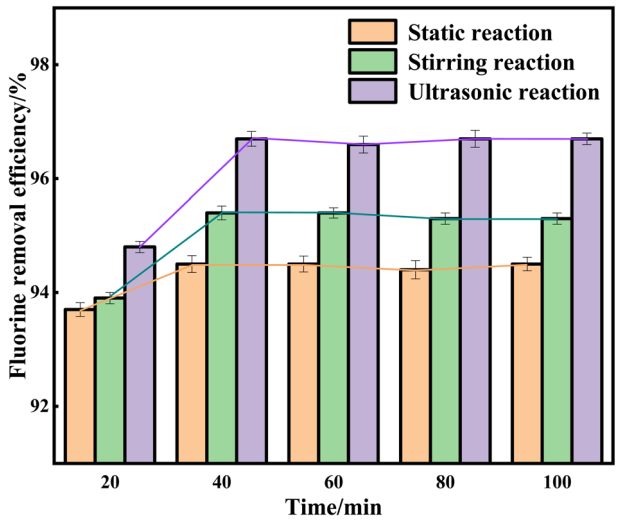

Fig. 5 The results under different reaction time.

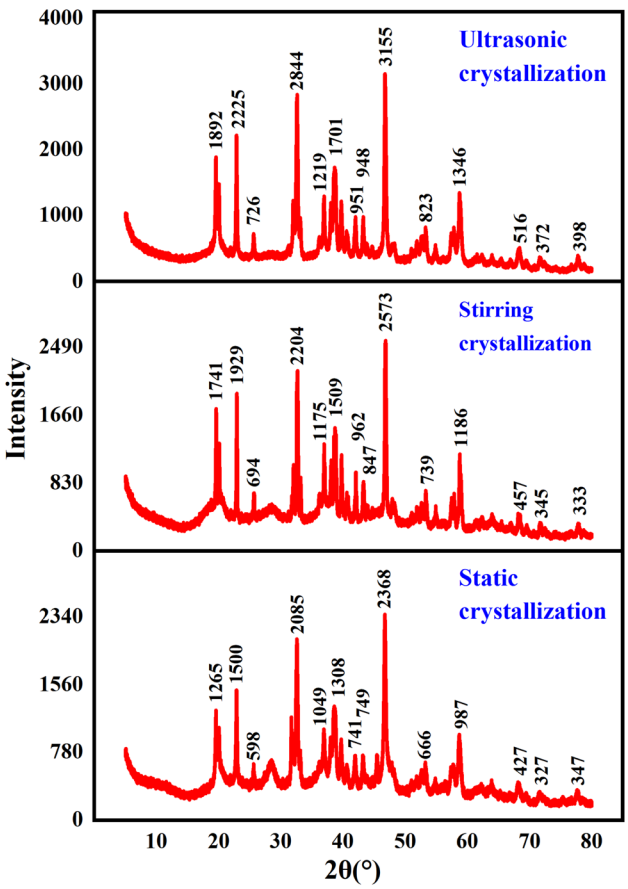

Fig. 6 XRD diagram of synthetic cryolite.

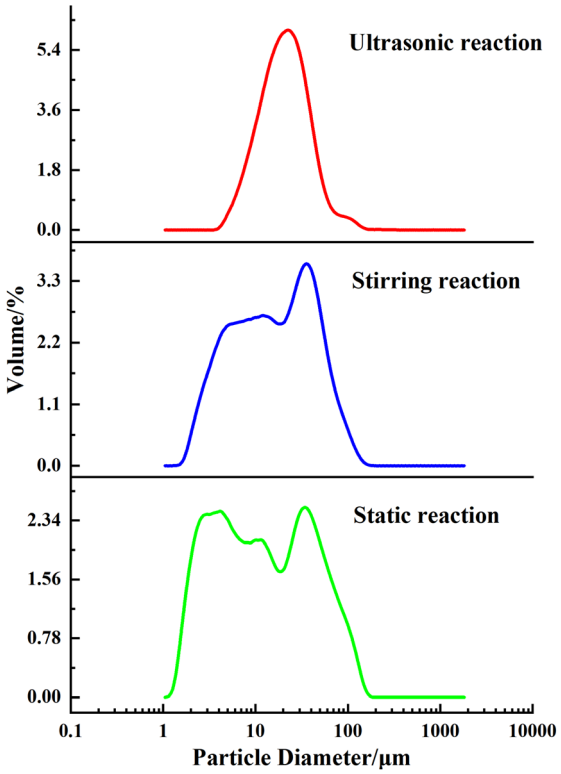

Fig. 7 Particle size distribution of cryolite.

flocculent, with a slower filtration rate. Usually, the solution has reached room temperature during the filtration process. Therefore, from the perspective of energy consumption, the optimal reaction temperature is determined to be 25 °C.

Since the precipitated cryolite is flocculated, it requires a certain amount of reaction time to aggregate into a cluster. If the time is not sufficient, the precipitation amount will be minimal. The effects of different reaction times on the removal efficiency of fluoride ions under three different reaction states were investigated. From Fig. 5, it can be seen that under the static reaction state, the removal efficiency of fluoride ions is the highest at 94.5% at a time of 40 minutes; under the stirring reaction state, the removal efficiency of fluoride ions is the highest at 95.4% when the time is 40 minutes; in the ultrasonic reaction state, when the time is 40 minutes, the removal efficiency of fluoride ions is the highest, at 96.7%. As shown in the figure, when the reaction time is 40 min, the reaction has reached saturation, and the removal efficiency of fluoride ions does not change much with the increase of reaction time.

3.2 Characterization of synthetic cryolite

The final XRD quantitative test was carried out on the solid materials synthesized under the optimal treatment conditions of fluoride containing wastewater. The results are shown in Fig. 6. The solid materials synthesized in the three states of

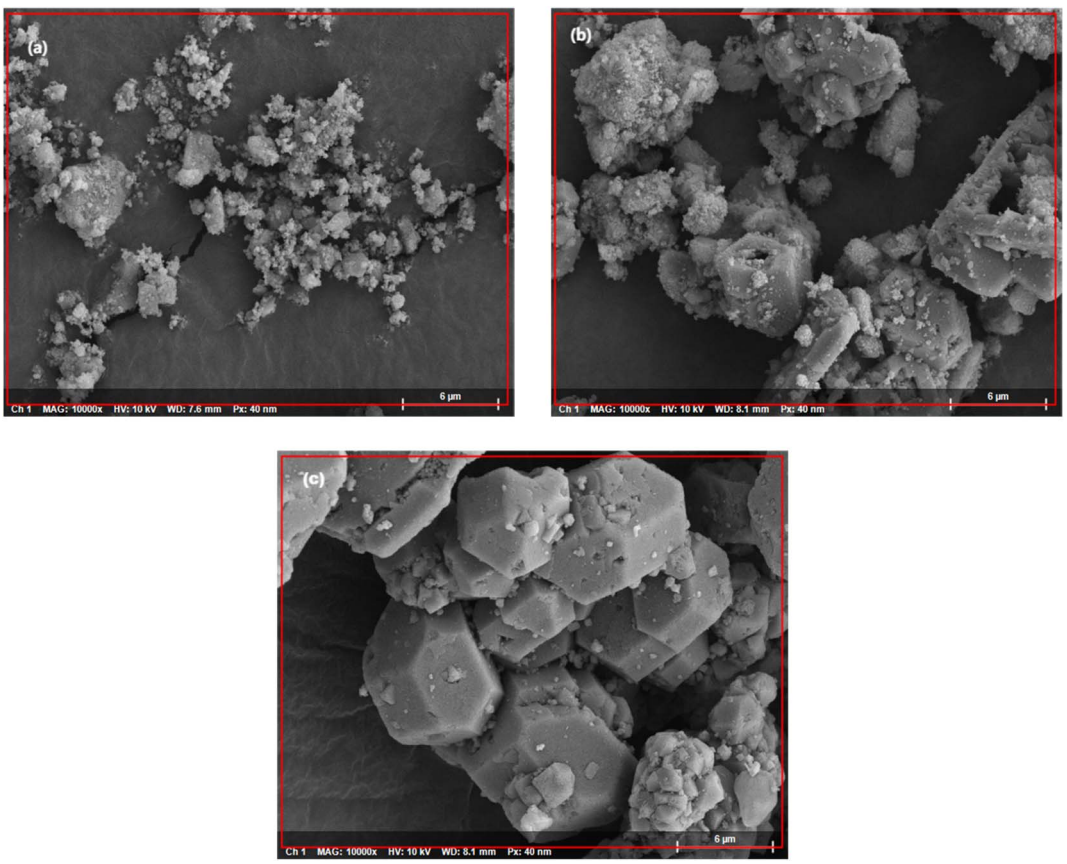

Fig. 8 SEM diagrams of synthetic cryolite: (a) static reaction; (b) stirring reaction; (c) ultrasonic reaction.

static reaction, stirring reaction and ultrasonic assisted reaction are all cryolite. It can be seen from the figure that the diffraction peaks corresponding to the three reaction states gradually increase, indicating that the crystal development tends to be good, and the content of cryolite gradually increases, which are 94.72%, 95.39% and 98.36%, respectively.

The particle size distribution of cryolite crystals synthesized under three reaction conditions was tested. It can be seen from Fig. 7 that ultrasonic has a significant effect on the particle size distribution of cryolite products. The product particles obtained by ultrasonic crystallization are uniform, and the particle size is concentrated in 10–50 μm, while the particle size of cryolite products obtained without ultrasonic is not uniform, and the particle size distribution is 4–90 μm.

The cryolite crystals synthesized under three different reaction states were characterized by SEM and TEM to observe their surface morphology and internal structure. As shown in Fig. 8 and 9. The relatively loose particles of cryolite recovered in the static state are of different sizes, and only a few particles have the tendency of aggregation and stacking. The recovered cryolites in the stirring state gradually gather together, and the surface of the cryolites gradually becomes smooth. The cryolite particles in the ultrasonic state are relatively regular, the surface is smooth and evenly distributed, the stacking is dense, and the crystallization is better.

Due to the fact that the quality of crystal formation depends on crystal growth rate, crystal size, and crystal shape, and ultrasound can have an impact on these three factors.[28] Studies have shown that,[29] when the crystal grows in solution, there will be two liquid layers on the surface of the crystal – the adsorption layer and the stationary liquid layer. The first step in the formation of the crystal is that the solute will pass through the stationary liquid layer to the adsorption layer, and then gather on the surface of the crystal. In the ultrasonic environment, the impact generated by the collapse of cavitation bubbles can shorten or even destroy the double liquid layer, improving the efficiency of solute molecules aggregation and growth towards the crystal plane. At the same time, the ultrasonic wave can also make the grain vibrate locally and prevent the crystal nucleus from sinking. Because the energy released by ultrasonic cavitation is much larger than the energy required for the growth of cryolite, crushing larger crystals, promoting the growth of small crystals, forming secondary crystallization, and reducing the radius of crystal nucleation. As a result, the initial crystal nucleus with vastly different sizes eventually become regular and uniform grains.[30]

3.3 Research on optimization of response surface method

As previously known, the crystallization performance is the best under ultrasonic conditions, and the content of cryolite is the

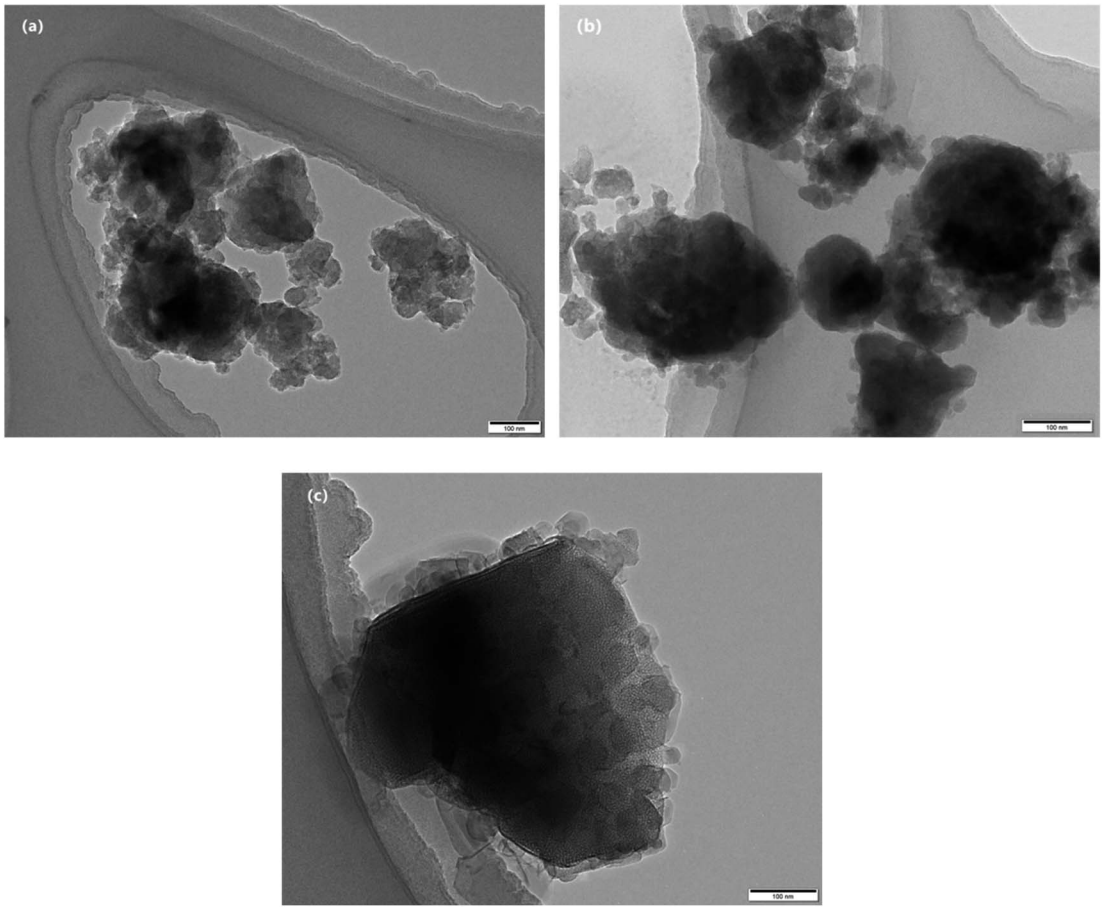

Fig. 9 TEM diagrams of synthetic cryolite: (a) static reaction; (b) stirring reaction; (c) ultrasonic reaction.

highest. In order to explore what factors play a dominant role, the Box–Behnken module in the Design Expert software was used to design the response surface test. The ultrasonic frequency, ultrasonic power and ultrasonic time were used as response factors, and the XRD quantitative analysis value $P(Na_3AlF_6)$ of cryolite was used as the response value. The influencing factors and levels of the test are shown in Table 2.

Table 2 Test influencing factors and levels

		Levels		
Factors	Variable	−1	0	1
Ultrasonic frequency/kHz	*A*	30	40	50
Ultrasonic power/W	*B*	420	480	540
Ultrasonic time/min	*C*	20	40	60

Table 3 Test design and response value

	Various factors and levels			
Test number	*A*	*B*	*C*	$P(Na_3AlF_6)$/%
1	30	480	20	95.4
2	40	420	60	98.36
3	50	420	40	98.4
4	50	480	60	98.31
5	40	540	20	96.9
6	30	480	60	97.4
7	40	480	40	98.38
8	40	480	40	98.37
9	30	540	40	97.69
10	40	480	40	98.36
11	40	420	20	96.1
12	50	480	20	96.3
13	40	540	60	98.45
14	50	540	40	98.35
15	30	420	40	97.1
16	40	480	40	98.35
17	40	480	40	98.36

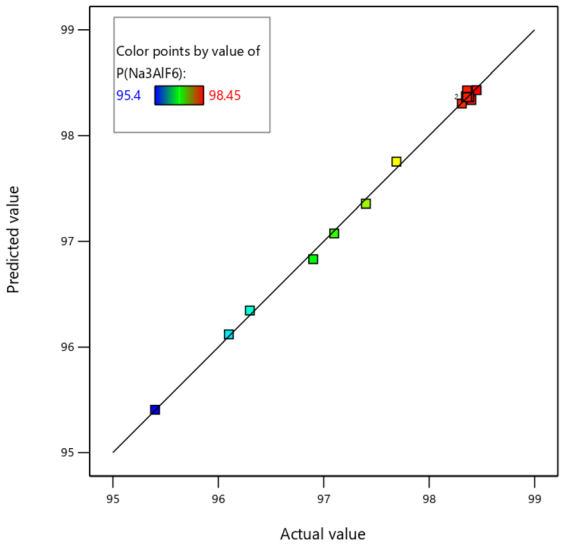

Fig. 10 Comparison curve between predicted value and actual value of cryolite content.

The XRD content of cryolite was used as the evaluation index, the Box–Behnken central combination module was used to design the influencing factors of the test to obtain 17 sets of tests. The test design scheme and results are shown in Table 3. It can be seen from Table 3 that the response value of cryolite content ranges from 94.5 to 98.45. The quadratic polynomial regression equation model is obtained by using Design Expert software to fit the data in Table 3, as shown in formula (3):

$$P = +98.36 + 0.4713A + 0.1788B + 0.9775C - 0.1600AB + 0.0025AC - 0.1775BC - 0.5395A^2 + 0.0605B^2 - 0.9720C^2 \quad (3)$$

In eqn (3): P is the content of cryolite; A is the ultrasonic frequency; B is ultrasonic power; C is the ultrasonic time.

Table 4 Regression model analysis of variance[a]

Variance source	Sum of squares	Degree of freedom	Mean square	*F*-Value	*q*-Value	Significance
Regression model	15.36	9	1.71	505.19	<0.0001	*
A	1.78	1	1.78	525.96	<0.0001	*
B	0.2556	1	0.2556	75.67	<0.0001	*
C	7.64	1	7.64	2262.99	<0.0001	*
AB	0.1024	1	0.1024	30.32	0.0009	*
AC	0.0000	1	0.0000	0.0074	0.9339	**
BC	0.1260	1	0.1260	37.31	0.0005	*
A^2	1.23	1	1.23	362.81	<0.0001	*
B^2	0.0154	1	0.0154	4.56	0.0700	**
C^2	3.98	1	3.98	1177.68	<0.0001	*
Residual	0.0236	7	0.0034			*
Lack of fit	0.0231	3	0.0077	59.29	0.0009	*
Pure error	0.0005	4	0.0001			
Cor total	15.38	16				
$R^2 = 0.9985$	$R_{adj}^2 = 0.9965$					

[a] * is significant difference ($q < 0.05$); ** is not significant difference ($q > 0.05$).

Analysis of variance was performed on the data, and the results are shown in Table 4. Among them, $q \leq 0.01$ is highly significant, and $q \leq 0.05$ is significant. It can be seen from Table 4 that the quadratic model $F = 505.19$ selected in this experiment shows that the constructed model is significant, $q < 0.0001$, indicating that the design is scientific and reasonable, the model is effective. There is a non-linear relationship between the influencing factors and the response values of each

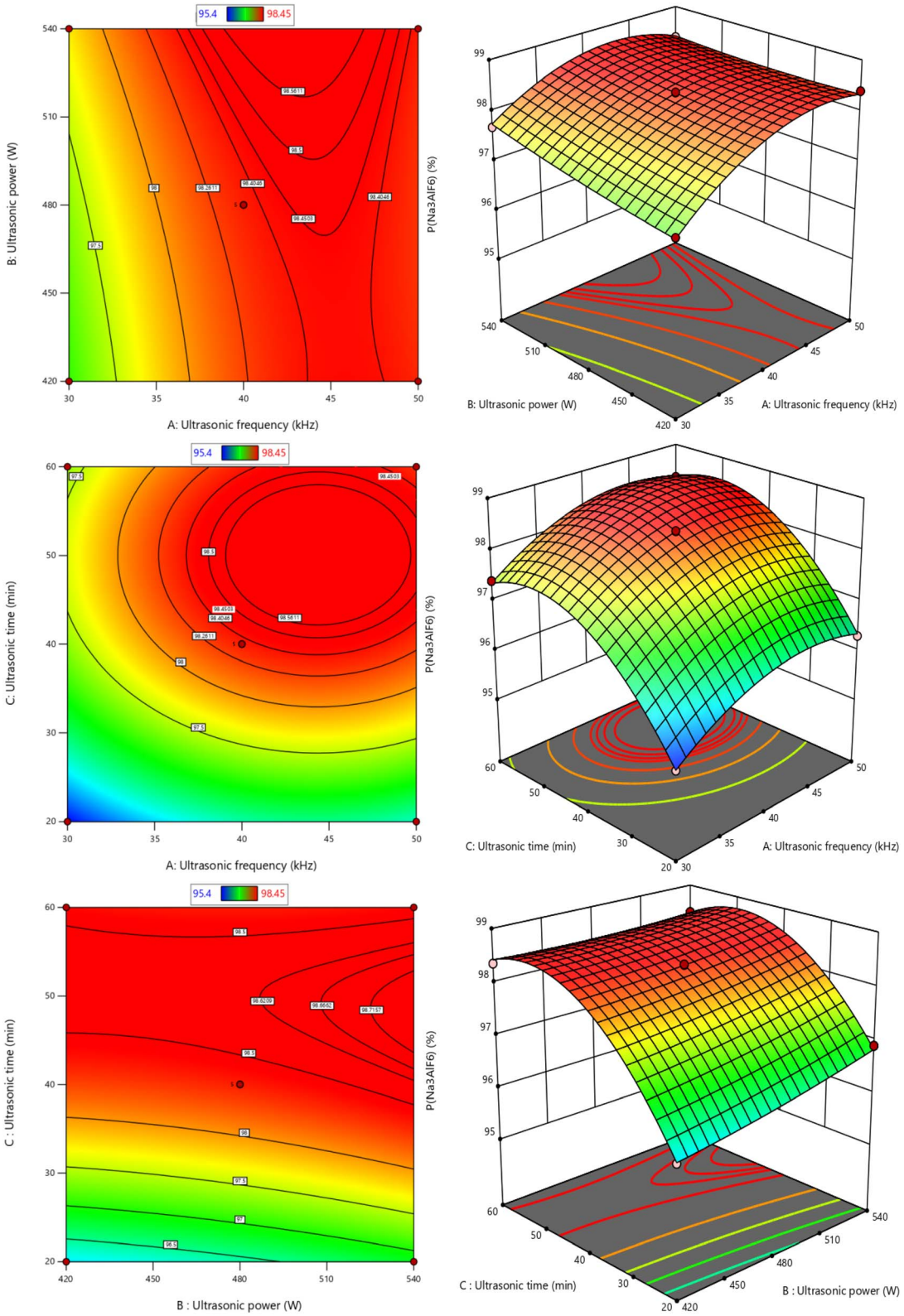

Fig. 11 Contour map and response surface graph of the interaction among three factors on cryolite content.

test. The equation $R^2 = 0.9985$, the correction coefficient $R_{adj}{}^2 = 0.9965$, the correlation coefficient is close to 1, indicating that 99.85% of the experimental data can be explained by this model in the experiment of optimizing the content parameters of cryolite by response surface method.

Fig. 10 is the reliability analysis diagram of the quadratic regression equation of the content of cryolite. The oblique line in the diagram shows the special case that the content of cryolite in the test is completely consistent with the predicted content of cryolite. It can be seen from the figure that the test values are concentrated on both sides of the slash and are close to the distance from the slash, indicating that the test and the expected model fit well.

The contour lines and response surface plots of the interaction between various factors was designed by Design-Expert software, as shown in Fig. 11. The projection of the response surface graph in the horizontal direction is a contour line. If the contour line is a gradient line or an ellipse, it indicates that the two factors have a very significant interaction. Contours are not significant if they are round. The steepness of the slope of the response surface of each factor reflects the degree of influence of this factor on the content of cryolite. The steeper the slope, the greater the influence. Therefore, based on the above analysis of contour lines and response surface plots, it can be concluded that the interaction between ultrasonic frequency and ultrasonic power, ultrasonic power and ultrasonic time is highly significant ($q < 0.01$), and the interaction of other factors is not significant. The single factor ultrasonic time has the most obvious influence on the content of cryolite, followed by ultrasonic frequency, and the least influence is ultrasonic power.

4. Conclusions

The crystallization method was used to treat fluoride containing wastewater generated during the treatment of spent cathode carbon from electrolytic aluminum. The removal efficiency of fluoride ions in the solution under three reaction conditions was compared. It was found that the removal efficiency of fluoride ions in the solution was the highest when $AlCl_3$ and NaCl were used as Al source and Na source respectively, the molar ratio of $AlCl_3$ to NaCl is 1 : 3, first addition of $AlCl_3$ and then NaCl, pH is 8.57, time is 40 min, and temperature at room temperature. Ultrasonic crystallization can significantly improve the content of cryolite, and the surface of cryolite is smooth and the particles are evenly distributed and concentrated. The response surface test showed that ultrasonic time has the most significant impact on the content of recovered cryolite among single factors, and the interaction between ultrasonic frequency and ultrasonic power, ultrasonic power and ultrasonic time was highly significant among multiple factors. This method provides a certain reference value for the effective synthesis and resource utilization of cryolite in electrolytic aluminum spent cathode carbon treatment wastewater.

Conflicts of interest

There is no conflict that needs to be declared.

Acknowledgements

We thank the National Key R&D Program of China (No. 2018YFC1903500) for financial support for this research.

References

1 L. F. Andrade, L. C. Davide and L. S. Gedraite, The effect of cyanide compounds, fluorides, aluminum, and inorganic oxides present in spent pot liner on germination and root tip cells of Lactuca sativa, *Ecotoxicol. Environ. Saf.*, 2010, **73**, 626–631, DOI: 10.1016/j.ecoenv.2009.12.012.

2 L. F. Andrade-Vieira, L. C. Davide and L. S. Gedraite, Genotoxicity of SPL (spent pot lining) as measured by Tradescantia bioassays, *Ecotoxicol. Environ. Saf.*, 2011, **74**, 2065–2069, DOI: 10.1016/j.ecoenv.2011.07.008.

3 J. Wang, H. Liu and Y. Luo, Study on Harmless and Resources Recovery Treatment Technology of Waste Cathode Carbon Blocks from Electrolytic Aluminum, *Procedia Environ. Sci.*, 2012, **16**, 769–777, DOI: 10.1016/j.proenv.2012.10.105.

4 D. F. Lisbona, C. Somerfield and K. M. Steel, Leaching of spent pot-lining with aluminium nitrate and nitric acid: effect of reaction conditions and thermodynamic modelling of solution speciation, *Hydrometallurgy*, 2013, **134–135**, 132–143, DOI: 10.1016/j.hydromet.2013.02.011.

5 Y. Xiao, L. Li and M. Huang, Treating waste with waste: Metals recovery from electroplating sludge using spent cathode carbon combustion dust and copper refining slag, *Sci. Total Environ.*, 2022, **838**, 156453, DOI: 10.1016/j.scitotenv.2022.156453.

6 Z. Yao, Q. Zhong and J. Xiao, An environmental-friendly process for dissociating toxic substances and recovering valuable components from spent carbon cathode, *J. Hazard. Mater.*, 2021, **404**, 124120, DOI: 10.1016/j.jhazmat.2020.124120.

7 Y. Yong, H. Jianhang and L. Yongkui, A new method for simultaneous separation and solidification of arsenic from arsenic-bearing gypsum sludge using waste carbon cathodes, *Sep. Purif. Technol.*, 2022, **291**, 120656, DOI: 10.1016/j.seppur.2022.120656.

8 L. Yegang, Environmental protection disposal of electrolytic aluminum waste electrode resources, *Shanxi Chem. Ind.*, 2023, **43**, 204–205, DOI: 10.16525/j.cnki.cn14-1109/tq.2023.07.082.

9 J. Xiao, J. Yuan and Z. Tian, Comparison of ultrasound-assisted and traditional caustic leaching of spent cathode carbon (SCC) from aluminum electrolysis, *Ultrason. Sonochem.*, 2018, **40**, 21–29, DOI: 10.1016/j.ultsonch.2017.06.024.

10 Z. Yao, Q. Zhong and J. Xiao, Efficient separation of fluoride and graphite carbon in spent cathode carbon from aluminum electrolysis by mechanical activation assisted alkali fusion treatment, *Miner. Eng.*, 2021, **161**, 106717, DOI: 10.1016/j.mineng.2020.106717.

11 J. Yuan, J. Xiao and F. Li, Co-treatment of spent cathode carbon in caustic and acid leaching process under

ultrasonic assisted for preparation of SiC, *Ultrason. Sonochem.*, 2018, **41**, 608–618, DOI: 10.1016/j.ultsonch.2017.10.027.

12 J. Lu and L. Zhang, Leaching Experimental Research on Fluorides in SPL of Aluminium Electrolysis, *Bull. Chin. Ceram. Soc.*, 2008, **27**, 634–639, DOI: 10.16552/j.cnki.issn1001-1625.2008.03.030.

13 Y. Ou and J. Zhu, Eluting fluorine from waste cathode carbon block by washing method, *Sci. Technol. Chem. Ind.*, 2019, **27**, 39–44, DOI: 10.3969/j.issn.1008-0511.2019.06.009.

14 J. Zhao and B. Zhang, Fluoride Leaching Test from Spent Pot Lining of Aluminum Electrolysis Cell, *Nonferrous Met., Extr. Metall.*, 2015, **3**, 30–36, DOI: 10.3969/j.issn.1007-7545.2015.03.008.

15 F. Yu, L. Jiang and Z. Li, Distribution, enrichment mechanisms, and health risk assessment of high-fluorine groundwater in the Yudong Plain, Henan Province, China, *Environ. Sci. Pollut. Res.*, 2023, **30**, 63549–63564, DOI: 10.1007/s11356-023-26765-0.

16 Z. Liu and X. Yu, Study on alkaline leaching and flotation process to deal with spent pot linings, *Light Met.*, 2012, **3**, 30–35, DOI: 10.3969/j.issn.1002-1752.2012.03.008.

17 C. Wang and S. Mao, Study on ultrasonic leaching and recovery of fluoride from spent cathode carbon of aluminum electrolysis, *RSC Adv.*, 2023, **13**, 16300–16310, DOI: 10.1039/d3ra02088f.

18 L. Yang, J. Zhou and Y. Feng, Treatment of fluorine-containing pharmaceutical wastewater by VUV/UV process, *Environ. Sci. Pollut. Res.*, 2022, **29**, 20289–20295, DOI: 10.1007/s11356-021-17063-8.

19 J. Park, H. Byun and W. Choi, Cement paste column for simultaneous removal of fluoride, phosphate, and nitrate in acidic wastewater, *Chemosphere*, 2008, **70**, 1429–1437, DOI: 10.1016/j.chemosphere.2007.09.012.

20 M. Guessous, A. Rich and S. Mountadar, Treatment of an industrial wastewater for phosphorus and fluoride recovery by a process coupling block freeze concentration and precipitation, *J. Cryst. Growth*, 2023, **619**, 127335, DOI: 10.1016/j.jcrysgro.2023.127335.

21 N. A. Tajuddin, E. F. B. Sokeri and N. A. Kamal, Fluoride removal in drinking water using layered double hydroxide materials: preparation, characterization and the current perspective on IR4.0 technologies, *J. Environ. Chem. Eng.*, 2023, **11**, 110305, DOI: 10.1016/j.jece.2023.110305.

22 Y. Li, L. Zhang and M. Liao, Removal of Fluoride from Aqueous Solution Using Shrimp Shell Residue as a Biosorbent after Astaxanthin Recovery, *Molecules*, 2023, **28**, 3897, DOI: 10.3390/molecules28093897.

23 Y. Ren and F. Wu, Extraction and preparation of metal organic frameworks from secondary aluminum ash for removal mechanism study of fluoride in wastewater, *J. Mater. Res. Technol.*, 2023, **23**, 3023–3034, DOI: 10.1016/j.jmrt.2023.01.198.

24 Y. Ren, M. He and G. Qu, Study on the mechanism of removing fluoride from wastewater by oxalic acid modified aluminum ash-carbon slag-carbon black doped composite, *Arabian J. Chem.*, 2023, **16**, 104668, DOI: 10.1016/j.arabjc.2023.104668.

25 A. Oulebsir, T. Chaabane and S. Zaidi, Preparation of mesoporous alumina electro-generated by electrocoagulation in NaCl electrolyte and application in fluoride removal with consistent regenerations, *Arabian J. Chem.*, 2020, **13**, 271–289, DOI: 10.1016/j.arabjc.2017.04.007.

26 S. Rajkumar, S. Murugesh and V. Sivasankar, Low-cost fluoride adsorbents prepared from a renewable biowaste: syntheses, characterization and modeling studies, *Arabian J. Chem.*, 2019, **12**, 3004–3017, DOI: 10.1016/j.arabjc.2015.06.028.

27 X. Meng and P. Zeng, Deep removal of fluoride from tungsten smelting wastewater by combined chemical coagulation-electrocoagulation treatment: from laboratory test to pilot test, *J. Cleaner Prod.*, 2023, **416**, 1374–1384, DOI: 10.1016/j.jclepro.2023.137914.

28 G. Zhichao and L. Hong, Effect of ultrasound on the crystallization and its mechanism, *Tianjin Chem. Ind.*, 2003, **17**, 1–4, DOI: 10.3969/j.issn.1008-1267.2003.03.001.

29 H. Li and H. Li, The application of power ultrasound to reaction crystallization, *Ultrason. Sonochem.*, 2006, **13**, 359–363, DOI: 10.1016/j.ultsonch.2006.01.002.

30 A. Markande, A. Nezzal and J. Fitzpatrick, Influence of impurities on the crystallization of dextrose monohydrate, *J. Cryst. Growth*, 2012, **353**, 145–151, DOI: 10.1016/j.jcrysgro.2012.04.021.